2.6. Statistical analysis

All data were statistically evaluated with StatView Ver. 4.50 (Abacus Concepts Inc., Berkeley, CA). The mRNA levels relative to β-actin mRNA levels in the various treatment groups were subject to one-way analyses of variance (ANOVA) followed by Scheffe's F-test. The optical density of immunoreactive bands was analyzed using Student's t-test. A probability (P) of less than 0.05 was considered significant in this study.

3. Results

Ethidium bromide staining of a polyacrylamide gel revealed a single band at the expected size of amplification product for each of the β-actin and the Homer cDNAs. Since no amplified products were observed when the reverse transcriptase step was omitted, the contamination by genomic DNA did not interfere with the signals of PCR products of Homer 1a, 1b and 1c cDNAs. The contamination by genomic DNA did not interfere with the signals of PCR products of β-actin, Homer 1b and Homer 1c, because these cDNAs were amplified using the pair of primers derived from different exons of the genes.

To determine the optimal amplifications, PCR was performed using different amount of reverse-transcribed total RNA and different numbers of cycles. The results indicated that amplification was exponential between 18 and 24 cycles for β-actin mRNA. Amplification was also exponential between 24 and 30 cycles for Homer 1a and 1c mRNAs. The PCR products were proportional to RNA input over a range of 5–50 ng total RNA for β-actin and Homer mRNAs. Twenty-five nanograms of reverse-transcribed RNA were amplified for 28 cycles for the quantitation of relative amount of the Homer mRNAs in the rat brain.

Acute administration of methamphetamine (40 mg/kg, i.p.) significantly increased Homer 1a mRNA levels in the striatum at 1 h (+66% of the pre-drug basal levels, $F_{3,30} = 6.48$, $P < 0.01$), 2 h (+155%, $F_{3,30} = 35.3$, $P < 0.001$) and 4 h (+84%, $F_{3,30} = 35.3$, $P < 0.001$) after methamphetamine (Fig. 1). Homer 1a mRNA levels were also increased significantly in the nucleus accumbens at 1 h (+60%, $F_{3,32} = 3.26$, $P < 0.05$) and 2 h (+94%, $F_{3,32} = 8.01$, $P < 0.01$) after methamphetamine. Methamphetamine did not affect Homer 1a mRNA levels in the medial prefrontal cortex and substantia nigra. The rank order of the density of Homer 1a mRNA was as follows: the striatum > medial prefrontal cortex > nucleus accumbens > substantia nigra (Fig. 1). The level of Homer 1a mRNA in the striatum was a fivefold higher than that in the substantia nigra.

Homer 1b mRNA levels could be detected in the substantia nigra, but not in other regions examined, under the standard experimental condition, while Homer 1c mRNA were detected with homogeneous distribution in all brain regions examined. Acute administration of methamphetamine (40 mg/kg, i.p.) did not affect gene expression of Homer 1b or 1c in any brain regions (Table 1).

As shown in Fig. 2, Homer 1a protein in the striatum migrated with a band of the molecular weight of 30 kDa estimated using prestained molecular weight marker. Quanti-

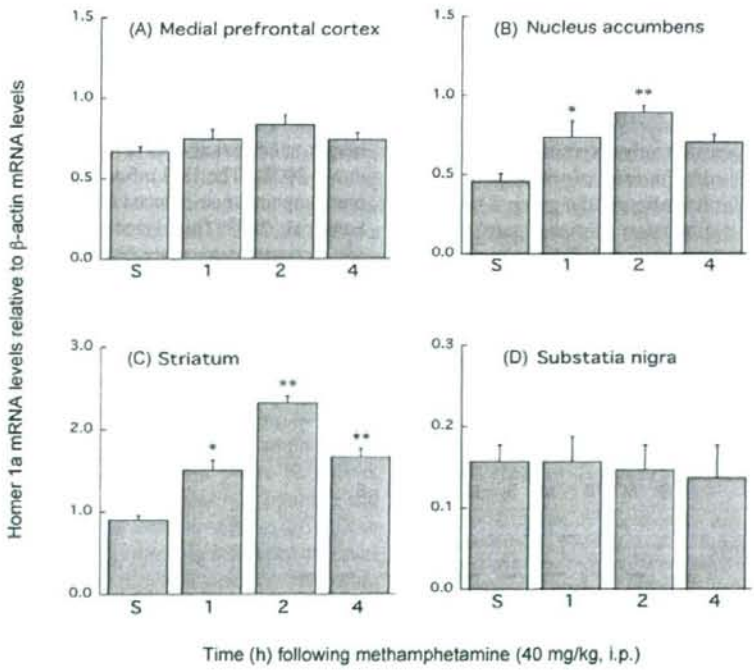

Fig. 1. Time-dependent effects of a neurotoxic dose of methamphetamine on Homer 1a mRNA levels in the rat brain. Rats were killed 1, 2 or 4 h after a single injection of methamphetamine (40 mg/kg, i.p.). The values represent mean ± S.E.M. of nine animals. $^{*}P < 0.05$ and $^{**}P < 0.01$ compared with saline-treated groups (S) using Scheffe's F-test.

Table 1
Time-dependent effects of a neurotoxic dose of methamphetamine on the mRNA levels of Homer 1b and 1c in the discrete regions of rat brain

Gene and brain region	Homer mRNA levels relative to β-actin mRNA			
	Saline	Time (h) following methamphetamine (40 mg/kg, i.p.)		
		1	2	4
Homer 1b				
Substantia nigra	0.36 ± 0.07	0.35 ± 0.07	0.29 ± 0.03	0.33 ± 0.03
Homer 1c				
Medial prefrontal cortex	0.99 ± 0.05	0.85 ± 0.07	0.85 ± 0.10	0.81 ± 0.05
Nucleus accumbens	0.96 ± 0.13	0.95 ± 0.08	1.01 ± 0.06	0.97 ± 0.04
Striatum	1.17 ± 0.06	0.90 ± 0.09	0.88 ± 0.07	1.07 ± 0.04
Substantia nigra	0.92 ± 0.10	0.99 ± 0.15	0.88 ± 0.06	1.03 ± 0.14

Data are presented as mean ± S.E.M. of eight animals.

tative analysis of Western blot showed a small but significant increase in Homer 1a protein (+18%, d.f. = 18, $t = 2.61$, $P < 0.05$, Student's t-test, two-tailed) 4 h after administration of methamphetamine (40 mg/kg, i.p.). We replicated the same experiment independently and then also found a significant increase in the striatal Homer 1a protein (+23%, d.f. = 12, $t = 2.44$, $P < 0.05$, Student's t-test, two-tailed) (data not shown).

4. Discussion

The most striking finding of the present study was that methamphetamine induced gene expression of Homer 1a, but nor 1b or 1c, in the striatum and nucleus accumbens. These results further support the hypothesis that the induction of Homer 1a may play an important role in the dopamine–glutamate interaction in the basal ganglia.

Homer 1a selectively blocks binding of Homer 1b and 1c to the group 1 mGluRs (Xiao et al., 1998; Kato et al., 1998). Homer 1b and 1c are constitutively expressed and form a physical linking mGluRs with the inositol triphosphate (IP_3) receptors (Tu et al., 1998). Activation of the group 1 mGluRs, $mGluR_{1a}$ and $mGluR_5$, stimulates phospholipase C and generates IP_3, resulting in the release of Ca^{2+} from intracellular Ca^{2+} stores (Nakanishi, 1994). Therefore, Homer 1a may disrupt the coupling between mGluRs and IP_3 receptors and then inhibit glutamate-induced release of intracellular Ca^{2+}. Moreover, the expression of Homer 1a is reported to induce activation of $mGluR_{1a}$ and $mGluR_5$ (Ango et al., 2001). Our results suggest the methamphetamine-induced modification of excitatory synapse in the striatum and nucleus accumbens.

The dose employed in this study of methamphetamine (40 mg/kg) is sufficient to produce the methamphetamine-induced neurotoxicity to produce long-lasting depletion of contents, synthesis rate and transporter numbers of dopamine (Fukumura et al., 1998; Seiden and Ricaurte, 1987). Such a dose of methamphetamine induces hyperthermia and an excessive increase in extracellular dopamine levels reflected by a decrease in tissue dopamine levels in mice or rats at 1 to 4 h post-treatment of methamphetamine, all of which effects lead to dopaminergic deficits that is evident 24 h after and long persisted (Binienda et al., 2006; Fukumura et al., 1998; Thiriet et al., 2001). Simultaneously, methamphetamine induces expression of several genes in association with the dopaminergic neurotoxicity, as revealed by microarray studies (Xie et al., 2002). The IEG c-fos is also induced in relation to the methamphetamine-induced dopaminergic neurotoxicity (Nakahara et al., 2003; Thiriet et al., 2001) because null mutation of c-fos is reported to exacerbate the methamphetamine-induced dopaminergic deficits (Deng et al., 1999). Moreover, multiple

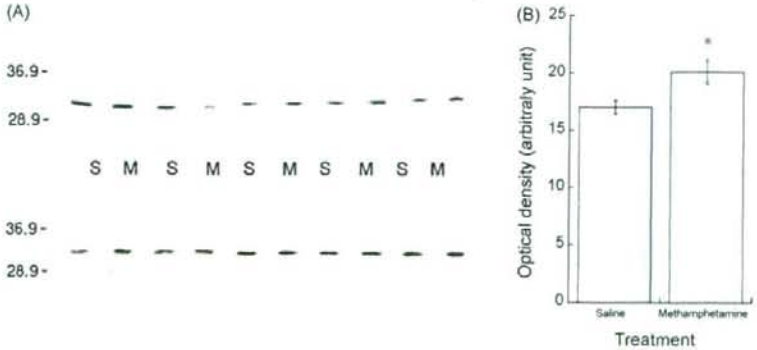

Fig. 2. Effect of a neurotoxic dose of methamphetamine on the protein expression of Homer 1a in rat striatum. (A) Photograph of Western blot of rat striatum obtained from saline (S) or methamphtamine (M) treatment group; (B) quantitative Western blot analysis. The values represent mean ± S.E.M. of 10 animals. $^*P < 0.05$ compared with saline-treated group using Student's t-test.

factors including hyperthermia, mitochondrial disruption, generation of reactive species, alterations of dopamine transporter and vesicular monoamine transporter-2 activities, and changes in glutamate signaling, have been thought to contribute to the methamphetamine-induced dopaminergic neurotoxicity (Riddle et al., 2006). Methamphetamine increases extracellular levels of not only dopamine but also glutamate in the striatum and nucleus accumbens, which may cause exicitoxicity that damages nerve terminals (Nash and Yamamoto, 1993; Xue et al., 1996), while the $mGluR_5$ antagonist prevents the methamphetamine-induced neurotoxicity in a temperature-independent manner (Battaglia et al., 2002). Taken into account with an interaction between Homer 1a and $mGluR_5$ as discussed earlier, the present results imply that the induction of Homer 1a expression may be involved at least in part in the methamphetamine-induced neurotoxicity. In this regard, Tappe and Kuner (2006) recently demonstrated that striosomal Homer 1a-expressing mice enhanced the amphetamine-induced stereotyped behavior as well as c-fos expression, suggesting a critical role of striosomal Homer 1a in dopaminergic responses to amphetamines. While c-fos expression in response to neurotoxic methamphetamine is observed widely throughout the various brain regions including prefrontal cortex and hippocampus (Thiriet et al., 2001), the present results demonstrate the region-specific induction of Homer 1a in the striatum and nucleus accumbens, of which dopamine terminals are most vulnerable to the neurotoxic effect of methamphetamine (Seiden and Ricaurte, 1987).

A high dose of methamphetamine is also known to exert a neurotoxic effect on serotonergic terminals in the cortical areas (Seiden and Ricaurte, 1987), while methamphetamine at the dose used in this study did not induce Homer 1a expression in the medial prefrontal cortex. In the prefrontal cortex, lysergic acid diethylamide (LSD), a hallucinogen displaying potent agonistic activity at serotonin–$5\text{-}HT_{2A}$ and/or $5\text{-}HT_{2C}$ receptors, is reported to increase mRNAs of the IEG Ania3, a splicing isoform of Homer 1a (Nichols and Sanders-Bush, 2002). The psychotomimetic phencyclidine that blocks NMDA receptor channels also induces Homer 1a in the same region (Cochran et al., 2002). Taken together with our previous data (Yamada et al., 2007), gene expression of Homer 1a in response to methamphetamine is likely to occur region-specifically in the striatum and nucleus accumbens that abundantly receive the dopaminergic projection from the substantia nigra pars compacta and ventral tegmental area, respectively.

Details of the mechanism by which methamphetamine induces gene expression of Homer 1a has yet to be known. Excessive increases in extracelluar levels of both dopamine and glutamate may be involved (Nash and Yamamoto, 1993; Xue et al., 1996). The striatal Homer 1a was induced to the maximal level 2 h after methamphetamine, which time-dependent profile is similar to that of Homer 1a induction with the dopamine D_1 receptor agonist SKF38393 (Berke et al., 1998; Yamada et al., 2007). Glutamate is reported to induce Homer 1a much slower (the maximal level at 4 h) in cerebellar granule cell culture (Sato et al., 2001). Moreover, activation of D_1 receptors may affect the methamphetamine-induced dopaminergic neurotoxicity due to induction of neuronal nitric oxide synthase mRNA expression in the striatum, which increases reactive species levels (Riddle et al., 2006). Therefore, the methamphetamine-induced D_1 receptor stimulation, as occurs following administration of methamphetamine, may induce Homer 1a mRNA in the striatum. It is most likely that activation of NMDA receptor by D_1 receptor stimulation contributes to Homer 1a expression because of a functional interaction between D_1 receptors and NMDA receptors for calcium signaling in the basal ganglia (Cepeda and Levine, 1998). Most of the G-protein coupled receptors including dopamine receptors and mGluRs may also share direct or indirect bindings with each other. However, it remains unclear whether a non-toxic dose (not more than 5 mg/kg) of methamphetamine induces or not Homer 1a expression. Further studies need to elucidate the molecular mechanism of Homer 1a induction under stimulated conditions.

Basal levels of Homer 1a mRNAs were higher in the forebrain regions than those in the midbrain. In contrast, Homer 1b mRNA levels were higher in the substantia nigra than those in other regions examined. Homer 1b allows translocation and clustering of $mGluR_5$ at dendritic synaptic sites, while the induction of Homer 1a expression triggers translocation of $mGluR_5$ from soma to dendrites (Ango et al., 2000; Tadokoro et al., 1999; Roche et al., 1999). Taken together with the present findings, the mGluRs may exist at axon and/or dendrites in the forebrain and at soma in the substantia nigra, respectively. The large amounts of Homer 1a induced in the striatum and nucleus accumbens may translocate the mGluRs at synaptic sites and enhance the excitability of the synapses after methamphetamine.

In conclusion, a neurotoxic dose of methamphetamine induced Homer 1a gene in the striatum and nucleus accumbens, but not in the medial prefrontal cortex, suggesting that the induction of Homer 1a gene may be associated at least in part with the methamphetamine-induced dopaminergic neurotoxicity. This finding may imply a possible involvement of Homer 1a in the pathophysiology of neurodegenerative diseases in the basal ganglia such as Parkinson disease.

References

Ango, F., Pin, J.-P., Tu, J.C., Xiao, B., Worley, P.F., Bockaert, J., Fang, L., 2000. Dendritic and atonal targeting of type 5 metabotropic glutamate receptor is regulated by Homer 1 proteins and neuronal excitation. J. Neurosci. 20, 8710–8716.

Ango, F., Prezeau, L., Muller, T., Tu, J.C., Xiao, B., Worley, P.F., Pin, J.P., Bockaert, J., Frgni, L., 2001. Agonist-independent activation of metabotropic glutamate receptors by the intracellular protein Homer. Nature 411, 962–965.

Battaglia, G., Fornai, F., Busceti, C.L., Aloisi, G., Cerrito, F., De Blasi, A., Melchiorri, D., Nicoletti, F., 2002. Selective blockade of mGlu5 metabotropic glutamate receptors is protective against methamphetamine neurotoxicity. J. Neurosci. 22, 2135–2141.

Berke, J.D., Paletzki, R.F., Aronson, G.J., Hyman, S.E., Gerfen, C.R., 1998. A complex program of striatal gene expression induced by dopaminergic stimulation. J. Neurosci. 18, 5301–5310.

Binienda, Z.K., Przybyla, B.D., Robinson, B.L., Salem, N., Virmani, A., Amato, A., Ali, S., 2006. Effects of L-carnitine pretreatment in methamphetamine and 3-nitropropionic acid-induced neurotoxicity. Ann. N. Y. Acad. Sci. 1074, 74–83.

Bottai, D., Guzowski, J.F., Schwarz, M.K., Kang, S.H., Xiao, B., Lanahan, A., Worley, P.F., Seeburg, P.H., 2002. Synaptic activity-induced conversion of intronic to exonic sequence in Homer 1 immediate early gene expression. J. Neurosci. 22, 167–175.

Brakeman, R.P., Lanahan, A.A., O'Brien, R., Roche, K., Barnes, C.A., Huganir, R.L., Worley, P.F., 1997. Homer: a protein that selectively binds metabotropic glutamate receptors. Nature 386, 284–288.

Cepeda, C., Levine, M.S., 1998. Dopamine and *N*-methyl-D-aspartate receptor interactions in the neostriatum. Dev. Neurosci. 20, 1–18.

Carlsson, M., Carlsson, A., 1990. Interactions between glutamatergic and monoaminergic systems within the basal ganglia-implications for schizophrenia and Parkinson's disease. Trends Neurosci. 13, 272–276.

Chomczynski, P., Sacchi, N., 1987. Single-step method of RNA isolation by acid guanidinium thiocyanate-phenol-chloroform extraction. Anal. Biochem. 162, 156–159.

de Bartolomeis, A., Alojo, L., Ambesi-Impiombato, A., Bravi, D., Caraco, C., Muscettola, G., Barone, P., 2002. Acute administration of antipsychotics modulates Homer striatal gene expression differentially. Mol. Brain Res. 98, 124–129.

Cochran, S.M., Fujimura, M., Morris, B.J., Pratt, J., 2002. Acute and delayed effects of phencyclidine upon mRNA levels of markers of glutamatergic and GABAergic neurotransmitter function in the rat brain. Synapse 46, 206–214.

Deng, X., Ladenheim, B., Tsao, L.-I., Cadet, J.L., 1999. Null mutation of c-fos causes exacerbation of methamphetamine-induced neurotoxicity. J. Neurosci. 19, 10107–10115.

Fukumura, M., Cappon, G.D., Pu, C., Broening, H.W., Vorhees, C.V., 1998. A single dose model of methamphetamine-induced neurotoxicity in rats: effects on neostriatal monoamines and glial fibrillary acidic protein. Brain Res. 806, 1–7.

Gotoh, L., Kawanami, N., Nakahara, T., Hondo, H., Motomura, K., Ohta, E., Kanchiku, I., Kuroki, T., Hirano, M., Uchimura, H., 2002. Effects of the adenosine A_1 receptor agonist N^6-cyclopentyladenosine on phencyclidine-induced behavior and expression of the immediate-early genes in the discrete brain regions of rats. Mol. Brain Res. 100, 1–12.

Kato, A., Ozawa, F., Saitoh, Y., Fukazawa, Y., Sugiyama, H., Inokuchi, K., 1998. Novel members of the Vesl/Homer family of PDZ proteins that bind metabotropic glutamate receptors. J. Biol. Chem. 273, 23969–23975.

Kato, A., Ozawa, F., Saitoh, Y., Hirai, K., Inokuchi, K., 1997. Vesl, a gene encoding VASP/Ena family related protein, is upregulated during seizure, long-term potentiation and synaptogenesis. FEBS Lett. 412, 183–189.

Morari, M., Marti, M., Sbrenna, S., Fuxe, K., Bianchi, C., Beani, L., 1998. Reciprocal dopamine-glutamate modulation of release in the basal ganglia. Neurochem. Int. 33, 383–397.

Morioka, R., Kato, A., Fueta, Y., Sugiyama, H., 2001. Expression of vesl-1S/homer-1a, a gene associated with long-term potentiation, in the brain of the epileptic El mouse. Neurosci. Lett. 313, 99–101.

Nakahara, T., Hirano, M., Matsumoto, T., Kuroki, T., Tatebayashi, Y., Tutsumi, T., Nishiyama, K., Ooboshi, H., Nakamura, K., Yao, H., Shiraishi, A., Waki, M., Uchimura, H., 1990. Regional distribution of DNA and RNA in rat brain: a sensitive determination using high-performance liquid chromatography with electrochemical detection. Neurochem. Res. 15, 609–611.

Nakahara, T., Hunter, R.J., Preedy, V.R., Martin, C.R., Reilly, M.E., 2005. Practical method for determining mRNA levels in alcohol-exposed tissues and its application to experimental pathology. In: Preedy, V., Watson, R. (Eds.), Comprehensive Handbook of Alcohol Related Pathology, vol. 3. Elsevier, London, pp. 1611–1618.

Nakahara, T., Kuroki, T., Ohta, E., Kajihata, T., Yamada, H., Yamanaka, M., Hashimoto, K., Tsutsumi, T., Hirano, M., Uchimura, H., 2003. Effect of the neurotoxic dose of methamphetamine on gene expression of Parkin and Pael-receptors in rat striatum. Parkinsonism Related Disord 9, 213–219.

Nakanishi, S., 1994. Metabotropic glutamate receptors: synaptic transmission, modulation, and plasticity. Neuron 13, 1031–1037.

Nash, J.F., Yamamoto, B.K., 1993. Effect of d-amphetamine on the extracellular concentrations of glutamate and dopamine in iprindole-treated rats. Brain Res. 627, 1–8.

Nichols, C.D., Sanders-Bush, E., 2002. A single dose of lysergic acid diethylamide influences gene expression patterns within the mammalian brain. Neuropsychopharmacology 26, 634–642.

Nielsen, H.S., Georg, B., Hannibal, J., Fahrenkrug, J., 2002. Homer-1 mRNA in the rat suprachiasmatic nucleus is regulated differentially by the retinohypothalamic tract transmitters pituitary adenylate cyclase activating polypeptide and glutamate at time points where light phase-shifts the endogenous rhythm. Mol. Brain Res. 105, 79–85.

Park, H.T., Kang, E.K., Bae, K.W., 1997. Light regulates Homer mRNA expression in the rat suprachiasmatic nucleus. Mol. Brain Res. 52, 318–322.

Polese, D., de Serpis, A.A., Ambesi-Impiombato, A., Muscettola, G., de Bartolomeis, A., 2002. Homer 1a gene expression modulation by antipsychotic drugs: involvement of the glutamate metabotropic system and effects of D-cycloserine. Neuropsychopharmacology 27, 906–913.

Riddle, E.L., Fleckenstein, A.E., Hanson, G.R., 2006. Mechanism of methamphetamine-induced dopaminergic neurotoxicity. AAPS J. 8, E413–E418.

Roche, K.W., Tu, J.C., Petralia, R.S., Xiao, B., Wenthold, R.J., Worley, P.F., 1999. Homer 1b regulates the trafficking of group I metabotropic glutamate receptors. J. Biol. Chem. 274, 25953–25957.

Sato, M., Suzuki, K., Nakanishi, S., 2001. NMDA receptor stimulation and brain-derived neurotrophic factor upregulate Homer 1a via mitogen-activated protein kinase cascade in cultured cerebellar granule cells. J. Neurosci. 21, 3797–3805.

Seiden, L.S., Ricaurte, G.A., 1987. Neurotoxicity of methamphetamine and related drugs. In: Meltzer, H.Y. (Ed.), Psychopharmacology: The Third Generation of Progress. Raven Press, New York, pp. 359–366.

Swanson, C.J., Baker, D.A., Carson, D., Worley, P.F., Kalivas, P.W., 2001. Repeated cocaine administration attenuates group I metabotropic glutamate receptor-mediated glutamate release and behavioral activation: a potential role for Homer. J. Neurosci. 21, 9043–9052.

Szumlinski, K.K., Lominac, K.D., Kleschen, M.J., Oleson, E.B., Dehoff, M.H., Schwarz, M.K., Seeburg, P.H., Worley, P.F., Kalivas, P.W., 2005. Behavioral and neurochemical phenotyping of Homer1 mutant mice: possible relevance to schizophrenia. Genes Brain Behav. 4, 273–288.

Tadokoro, S., Tachibana, T., Imanaka, T., Nishida, W., Sobue, K., 1999. Involvement of unique lucien-zipper motif of PSD-Zip45 (Homer 1c/vesl-1L) in group I metabotropic glutamate receptor clustering. Proc. Natl. Acad. Sci. USA 96, 13801–13806.

Tappe, A., Kuner, R., 2006. Regulation of motor performance and striatal function by synaptic scaffolding proteins of the Homer1 family. Proc. Natl. Acad. Sci. USA 103, 774–779.

Thiriet, N., Zwiller, J., Ali, S.F., 2001. Induction of the immediate early genes egr-1 and c-fos by methamphetamine in mouse brain. Brain Res. 919, 31–40.

Tu, J.C., Xiao, B., Yuan, J.P., Lanahan, A.A., Leoffert, K., Li, M., Linden, D.J., Worley, P.F., 1998. Homer binds a novel proline-rich motif and links group 1 metabotropic glutamate receptors with IP3 receptors. Neuron 21, 717–726.

Vandershuren, L.J., Kalivas, P.W., 2000. Alterations in dopaminergic transmission in the induction and expression of behavioral sensitization: a critical review of preclinical studies. Psychopharmacology 151, 99–120.

Xiao, B., Tu, J.C., Petralia, R.S., Yuan, J.P., Doan, A., Breder, C.D., Ruggiero, A., Lanahan, A.A., Wenthold, R.J., Worley, P.F., 1998. Homer regulates the association of group 1 metabotropic glutamate receptors with multivalent complexes of Homer-related, synaptic proteins. Neuron 21, 707–716.

Xie, T., Tong, L., Barrett, T., Yuan, J., Hatzidimitriou, G., McCann, U.D., Becker, K.G., Donovan, D.M., Ricaurte, G.A., 2002. Changes in gene expression linked to methamphetamine-induced dopaminergic neurotoxicity. J. Neurosci. 22, 274–283.

Xue, C.-J., Ng, J.P., Li, Y., Wolf, M.E., 1996. Acute and repeated systemic amphetamine administration: effects on extracellular glutamate, aspartate, and serine levels in rat ventral tegmental area and nucleus accumbens. J. Neurochem. 67, 352–363.

Yamada, H., Kuroki, T., Nakahara, T., Hashimoto, K., Tsutsumi, T., Hirano, M., Maeda, H., 2007. The dopamine D_1 receptor agonist, but not the D_2 receptor agonist, induces gene expression of Homer 1a in rat striatum and nucleus accumbens. Brain Res. 1131, 88–96.

Yano, M., Beverley, J.A., Steiner, H., 2006. Inhibition of methylphenidate-induced gene expression in the striatum by local blockade of D_1 dopamine receptors: interhemispheric effects. Neuroscience 140, 699–709.

Epilepsia, 49(9):1611–1618, 2008
doi: 10.1111/j.1528-1167.2008.01605.x

FULL-LENGTH ORIGINAL RESEARCH

Neural basis of photo/chromatic sensitivity in adolescence

***Takao Yamasaki, *†Yoshinobu Goto, ‡Naoko Kinukawa, and *Shozo Tobimatsu**

***Department of Clinical Neurophysiology, Neurological Institute, Graduate School of Medical Sciences, Kyushu University, Fukuoka, Japan; †Department of Occupational Therapy, Faculty of Rehabilitation, International University of Health and Welfare, Okawa, Japan; and ‡Department of Medical Information Science, Graduate School of Medical Sciences, Kyushu University, Fukuoka, Japan**

SUMMARY

Purpose: To determine a psychophysiological basis for age visual sensitivity to chromatic and achromatic stimuli.

Methods: We investigated the effects of achromatic and four isoluminant color combinations (blue/red, blue/green, green/red, and blue/yellow), luminance ratio changes in color combinations (blue/red; 1:1, 3:4, 4:3) and contrast changes (3 to 100%) on steady-state electroretinograms (ERGs) and visual evoked potentials (VEPs) in 32 healthy teenagers and 30 young adults.

Results: We found that (1) dual peaks at 9 and 18 Hz with a dip at 12 Hz were observed in VEPs with all isoluminant color combinations, (2) VEP responses were significantly enhanced and the 12-Hz dip became unclear with luminance ratio changes between two colors with a nonantagonistic relationship (blue/red), and (3) VEP amplitudes were significantly increased when the contrast was increased. These characteristics were more evident in teenagers than young adults; however, ERGs were qualitatively similar between the two groups.

Discussion: The visual cortex is differently modulated by different color-luminance combinations, and higher sensitivity to color-luminance combinations in the visual cortex in teenagers is responsible for the high prevalence of photo/chromatic sensitivity in adolescence.

KEY WORDS: Adolescence, Photo/chromatic sensitivity, Color-luminance combination, Visual evoked potentials, Visual cortex.

Photosensitive epilepsy (PSE) is a well-known condition characterized by seizures in patients who show photoparoxysmal responses (PPRs) on EEG elicited by intermittent photic stimulation (Harding & Jeavons, 1994; Kasteleijin-Nolst Trenité, 1998). On the other hand, photosensitivity is defined by abnormal EEG responses to light or pattern stimulation, and consisting of a PPR (Fisher et al., 2005). The estimated prevalence of seizures from light stimuli is ~1 per 10,000, or 1 per 4,000 individuals age 5–24 years, while photosensitivity occurs in ~0.3–3% of the population (Fisher et al., 2005). Television (TV) is the most common provocative stimulus for PSE (Parra et al., 2005). For example, a UK TV commercial film precipitated epileptic seizures in three viewers in 1993 (Fisher et al., 2005). In 1997, 685 Japanese children suffered epileptic seizures while watching a popular animated TV program (Pocket Monsters: Pokemon) (Harding, 1998; Hayashi et al., 1998; Tobimatsu et al., 1999). The key scenes in that program consisted of rapid blue/red (B/R) frame changes (temporal frequency, 12 Hz; luminance ratio, B:R = 4:3) (Harding, 1998; Tobimatsu et al., 1999). Interestingly, 76% of patients having "Pokemon seizures" had no previous history of epilepsy (Fisher et al., 2005), and 81% of these had no recurrence of epileptic seizures in a 5-year follow-up study (Okumura et al., 2004). Thus, healthy people can suffer from seizures induced by visual images. Therefore, it is important to examine the neural basis of latent color-luminance sensitivity in healthy people to prevent epileptic seizures occurring when watching TV.

Accepted March 4, 2008; Early View publication April 10, 2008.

Address correspondence to Takao Yamasaki, M.D., Ph.D., Department of Clinical Neurophysiology, Neurological Institute, Graduate School of Medical Sciences, Kyushu University, 3-1-1 Maidashi, Higashi-ku, Fukuoka 812-8582, Japan. E-mail: yamasa@neurophy.med.kyushu-u.ac.jp

Takao Yamasaki and Yoshinobu Goto contributed equally to the present paper.

Wiley Periodicals, Inc.
© 2008 International League Against Epilepsy

Several lines of evidence suggest that photosensitivity (Jeavons et al., 1972; Panayiotopoulos et al., 1972; Harding et al., 1975), pattern sensitivity (Wilkins et al., 1979; Harding et al., 1994; Fylan & Harding, 1997; Funatsuka et al., 2001) and temporal frequency dependence (Harding et al., 1994; Harding & Harding, 1999) play important roles in the generation of PSE. Our previous study (Tobimatsu et al., 1999) demonstrated that PPR is more frequently observed in response to rapid B/R frame changes (temporal frequency, 12 Hz) compared with monochromatic changes in the patients with "Pokemon seizure." No antagonistic relation exists between red and blue cone impulses in the primary visual cortex (V1) (Livingstone & Hubel, 1984), so B/R inputs result in maximal stimulation of the visual cortex. Therefore, we proposed chromatic sensitive epilepsy as a variant of PSE (Tobimatsu et al., 1999). However, it remains unknown how the visual cortex in healthy people responds to color-luminance stimuli.

In the present study, we focused on the neural basis of color-luminance sensitivity in healthy people; therefore, we investigated the effects of isoluminant color combinations, luminance ratio changes in color combinations and contrast changes on steady-state electroretinograms (ERGs) and visual evoked potentials (VEPs) in healthy teenagers and young adults. EEG was also monitored during the ERG and VEP recordings.

METHODS

Subjects

Thirty-two healthy teenagers (17 males and 15 females, aged 12–16 years) and 30 healthy young adults (18 males and 12 females, aged 23–40 years) were studied in different combinations in the four experiments. We defined healthy subjects as those with no color blindness by Ishihara color plates (Ishihara, 1997), no loss of visual acuity, no family history of epilepsy, no history of a febrile convulsion, and no neurological disorders. Informed consent was obtained after the nature of the experiment had been fully explained. The experimental procedures were approved by the ethics committee of the Graduate School of Medical Sciences, Kyushu University.

Visual stimuli

The stimuli were generated by a VSG Three (Cambridge Research Systems, Cambridge, U.K.) and displayed on a gamma-corrected color monitor with a frame rate of 100 Hz (GDM-17SE2T, SONY, Tokyo, Japan). We used achromatic (black/white, Bk/W) stimulation and four isoluminant color combination stimuli [no antagonistic color (blue/red, B/R and blue/green, B/G), and antagonistic color (green/red, G/R and blue/yellow, B/Y)] with a circular field of 10° at a viewing distance of 114 cm (Fig. 1A). CIE coordinates (measured by a Chromameter CS 100, Konica, Minolta, Tokyo, Japan) were $x = 0.391$, $y = 0.347$ (black); $x = 0.308$, $y = 0.342$ (white); $x = 0.290$, $y = 0.621$ (green); $x = 0.620$, $y = 0.353$ (red); $x = 0.166$, $y = 0.162$ (blue); $x = 0.422$, $y = 0.510$ (yellow). Figure 1B shows the wavelength sensitivity of cones, while Fig. 1C reveals the wavelength of each color in our stimuli measured by a photometer (Colormeter III F, KONICA MINOLTA, Tokyo, Japan), demonstrating that the wavelengths of B, G, and R were fitted to the peak spectral sensitivity of each cone. Visual stimuli were surrounded by a homogeneous background containing a mixture of color combinations (Fig. 1A). The mean luminance of the visual stimuli and

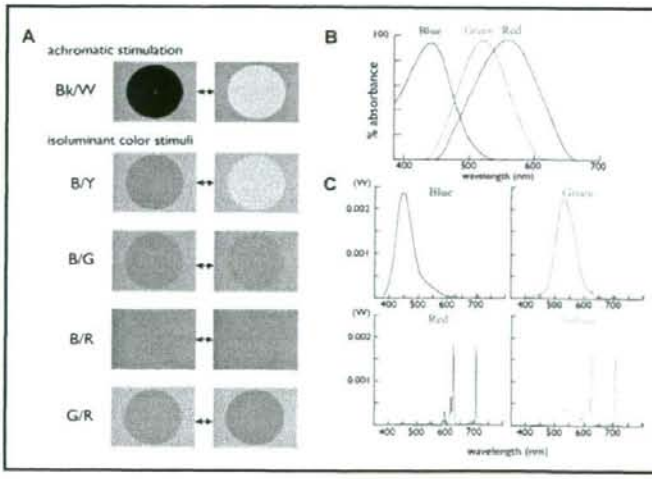

Figure 1.
Color combination stimuli used in this study. (**A**) shows achromatic [black/white (Bk/W)] and four isoluminant color combination stimuli [green/red (G/R), blue/red (B/R), blue/green (B/G), and blue/yellow (B/Y)] (visual angle, 10°; mean luminance, 24 cd/m^2). A fixation point (visual angle, 0.2°) is located in the center of the screen. Visual stimuli were surrounded by a homogeneous background with a mixture of two colors (mean luminance, 24 cd/m^2). (**B**) represents the wavelength sensitivity of cones, while (**C**) reveals the wavelength of each color measured by a photometer.
Epilepsia © ILAE

homogeneous background was 24 cd/m^2. Before the experiment, subjects viewed each color combination stimulus alternating at 15 Hz to establish psychophysical isoluminance, and adjusted the relative luminance to minimize perception of flicker.

All visual stimuli were presented for 30 s. First, the temporal frequency was varied from 3 to 24 Hz in 3-Hz steps to elucidate the temporal frequency characteristics of VEPs in response to achromatic and isoluminant chromatic stimulation. Second, the contrast of the stimuli was varied to study the effects of contrast changes. Bk/W and B/R stimuli were used and the temporal frequency was held constant at 12 Hz. Contrast was varied as follows: 3%, 5%, 10%, 20%, 30%, 40%, 60%, 80%, 90%, and 100%, with the mean luminance held constant at 24 cd/m^2. Achromatic contrast was defined as the Michaelson contrast: $(L\,\max - L\,\min)/(L\,\max + L\,\min)$, where Lmax is the maximum luminance and Lmin is the minimum luminance. Chromatic contrast was defined as $|r1 - r2|/(r1 + r2) = |b1 - b2|/(b1 + b2)$, and C1 = ($r1$, $g1$, $b1$) and C2 = ($r2$, $g2$, $b2$), where C1 and C2 represent each color in color combinations, and r, g, b are the elements of color. Third, the luminance ratio of the stimuli was varied to study the effect of luminance changes on color combinations. B/R and G/R stimuli were used, and their ratios were as follows: B (or G):R = 1:1, 4:3, 3:4. Subjects sat on a chair in a dark room, and fixated on a fixation point (visual angle 0.2°) in the center of the monitor. To prevent the triggering of a PPR during the experiment, only one eye was stimulated (Harding & Jeavons, 1994; Takahashi, 2002).

ERG, VEP, and EEG recordings

Steady-state ERGs were recorded from a surface skin electrode under the stimulated eye, referring to the electrode of the lateral orbital rim on the stimulated eye (Marmor et al., 2004). Pupils were not dilated. ERG recording was performed following the method of the International Society for Clinical Electrophysiology of Vision (Marmor et al., 2004). Steady-state VEPs were recorded from scalp electrodes placed over Oz, O1 and O2, referring to an electrode at Cz (International 10–20 system). The ground electrode was placed at Fz. Electrode impedance was maintained below 5 Kohm. The EEG signals were analog filtered between 0.5 and 200 Hz. EEG was also monitored during the ERG and VEP recordings using Neurofax EEG-1100 (Nihon Kohden, Tokyo, Japan).

Data analysis

The analog data were digitized at a sampling rate of 1000 Hz/channel and 15 samples of 2000 ms epoch were averaged using customized software (ERP average, Medical Try System, Tokyo, Japan). Epochs containing EEG deviations from the baseline greater than 100 μV were automatically rejected. The averaged responses were subjected to fast Fourier transform (FFT). The FFTs yielded the amplitude (square root of the power) of several harmonic components, but the first harmonic response (1F) was the most predominant. Thus, we mainly analyzed the 1F component. A three-way analysis of variance (ANOVA) with repeated measures was performed. Multiple comparisons with Bonferroni correction were also conducted for paired comparisons. For the contrast changes, analysis of covariance was performed.

Results

EEG monitoring

In both groups, EEG showed well-organized posterior dominant alpha activity (9–13 Hz) and no asymmetry in background activity. No spontaneous paroxysmal activity was observed. EEG showed photic-driving responses time-locked to the visual stimuli, however, no PPRs were found.

Different sensitivities to isoluminant color combinations in teenagers

Fig. 2 shows representative waveforms of VEPs to Bk/W stimulation from a teenager and a young adult, and their FFTs at each temporal frequency. VEPs were characterized by quasisinusoidal waveforms that corresponded to each temporal frequency. FFTs revealed that the first harmonic component (1F) was predominant. Fig. 3 shows the temporal frequency characteristics of the 1F amplitude to achromatic and color combination stimuli with no antagonistic relation (Fig. 3A, B) and with an antagonistic relation (Figs. 3C, D). Mean 1F amplitude in the teenagers was larger than that in young adults at all temporal frequencies in any color combination [$F(1,18) = 7.82$, $p < 0.01$]. The main effect of color combination stimuli was determined [$F(4,72) = 2.51$, $p < 0.05$]. In the teenagers, two amplitude peaks at 9 and 18 Hz with a dip at 12 Hz were observed in all color combinations (Figs. 3A, C). The amplitude of the 9-Hz peak was different among VEPs to color combinations ($p < 0.01$). The peak amplitude of Bk/W stimulation was the greatest and those of B/R and G/R were the lowest among the five color combinations. The 18-Hz peak of Bk/W and B/G stimuli tended to be larger than that of the other color combinations ($p = 0.061$). In contrast, young adults showed a 9-Hz peak, with a less defined 18-Hz peak due to low amplitudes (Figs. 3B, D). At the 9-Hz peak, the amplitude was greater with Bk/W stimulation than with the other color combinations ($p < 0.01$).

Higher sensitivities to contrast changes in teenagers

Fig. 4 shows the contrast modulation functions of VEP amplitudes to B/R and Bk/W stimuli in teenagers (Fig. 4A) and young adults (Fig. 4B). In both groups, VEPs showed a gradual increase in amplitude as a function of contrast in both stimuli [$F(1,396) = 112.2$, $p < 0.001$]; however,

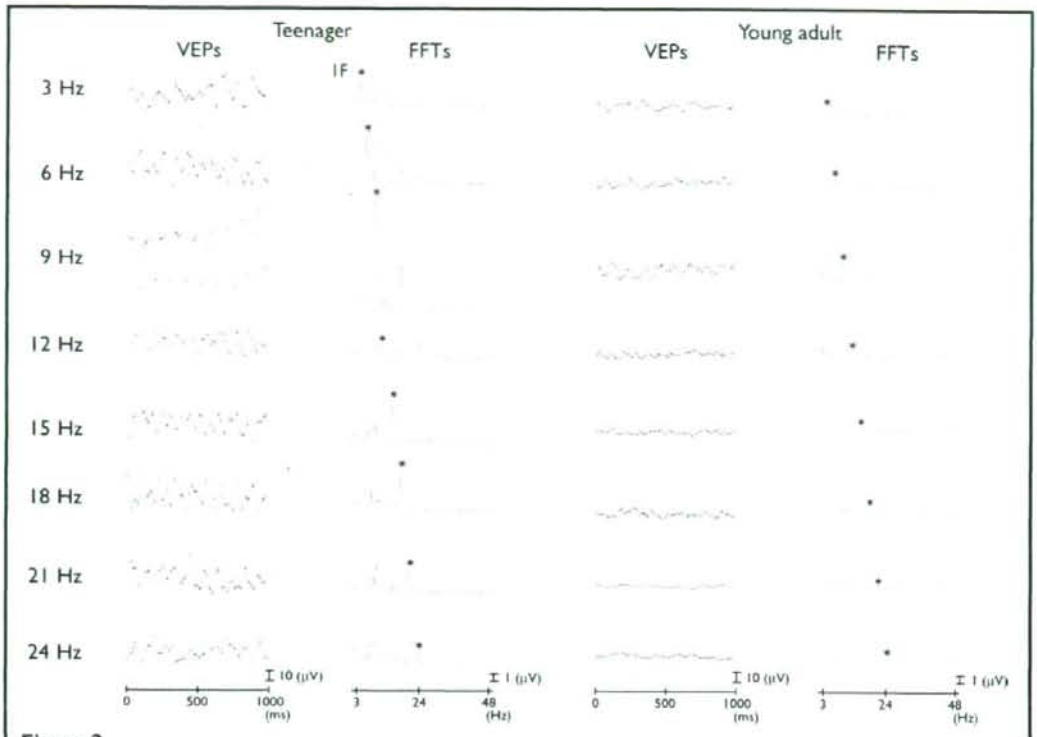

Figure 2.
Representative waveforms of VEPs and FFTs in response to Bk/W stimulation at each temporal frequency in a teenager and a young adult. Asterisks indicate the 1F. VEP amplitudes of the teenager are much larger than those of the young adult.
Epilepsia © ILAE

their slopes were much steeper in teenagers [$F(1,396) = 84.2$, $p < 0.001$]. These slopes tended to be saturated at about 40% with Bk/W stimulation and at about 80% with B/R stimulation in both groups. There was no significant difference in VEP amplitudes between the two stimuli in either group.

Luminance ratio changes in color combinations alter visual cortical responses

Figs. 5A and B show the response characteristics of VEP amplitudes to isoluminant and anisoluminant B/R stimuli. Mean VEP amplitude in teenagers was larger than that in young adults at all temporal frequencies of any color combination stimuli [$F(1,21) = 16.51$, $p < 0.005$]. Surprisingly, B/R with a low luminance of red ($B > R$) stimulation resulted in a larger amplitude and a less marked dip at 12 Hz compared with isoluminant B/R ($B = R$) stimulation in both teenagers ($p < 0.05$) and young adults ($p < 0.05$). In contrast, the VEP response to B/R with a high luminance of red ($B < R$) stimulation was lower than that of $B = R$ stimulation in teenagers ($p < 0.005$). In young adults, there was no difference in the VEP amplitude between $B < R$ and $B = R$ stimuli.

Figures 5C and D show the temporal frequency characteristics of VEP amplitudes to isoluminant and anisoluminant G/R stimuli. Mean VEP amplitude in teenagers was larger than that of young adults at all temporal frequencies of all color combinations [$F(1,21) = 11.07$, $p < 0.005$]. In the isoluminant G/R ($G = R$) condition, the dip at 12 Hz was less marked in both groups compared with the isoluminant B/R condition. In teenagers, G/R with a low luminance of red ($G > R$) stimulation resulted in a larger amplitude ($p < 0.005$) and no dip at 12 Hz compared with $G = R$ stimulation, while there were no differences in amplitude between $G > R$ and $G = R$ stimuli in young adults. In contrast, there were no differences in amplitude between G/R with a high luminance of red ($G < R$) and $G = R$ stimuli in both teenagers and young adults.

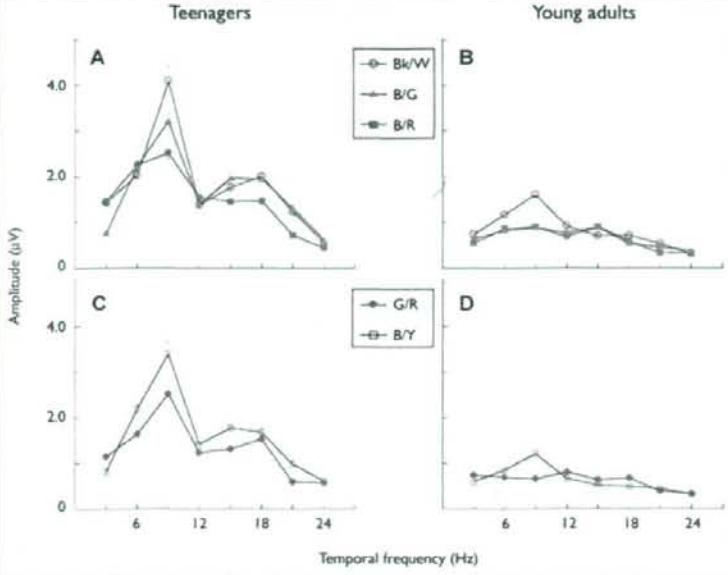

Figure 3.
Temporal frequency characteristics of VEP amplitudes in response to achromatic and isoluminant color combination stimuli in teenagers (n = 10) (**A, C**) and young adults (n = 10) (**B, D**). (**A, B**) show the response characteristics in achromatic and isoluminant color combination stimuli with no antagonistic relation, whereas (**C, D**) show those of isoluminant color combination stimuli with an antagonistic relation. Dual peaks at 9 and 18 Hz are evident in teenagers. Error bars represent S.E.M. in this and subsequent figures.
Epilepsia © ILAE

Differential effects of isoluminant color combinations on the retina and visual cortex

Mean 1F amplitudes of VEPs at 9 Hz were significantly larger than those of ERGs in both teenagers (n = 9) and young adults (n = 10) [$F(1,17) = 144.2$, $p < 0.001$]. VEP amplitudes in teenagers were again larger than those of young adults in any color combination ($p < 0.001$). The difference in VEP magnitude between color combinations was also found in teenagers ($p < 0.01$) and showed a trend in young adults ($p = 0.07$). In contrast, the difference in ERG amplitudes between teenagers and young adults was not significant. Furthermore, there was no difference in the order of ERG magnitude between color combinations in either teenagers or young adults.

Discussion

The visual sensitivities to color combinations, luminance ratio changes, and contrast changes are drastically changed around the age of 20 years. VEP differences were most pronounced in the isoluminant condition at 9 Hz, while there was no difference in ERG amplitudes in any color combinations between the two groups. It is likely that distinct visual sensitivities in teenagers are mainly related

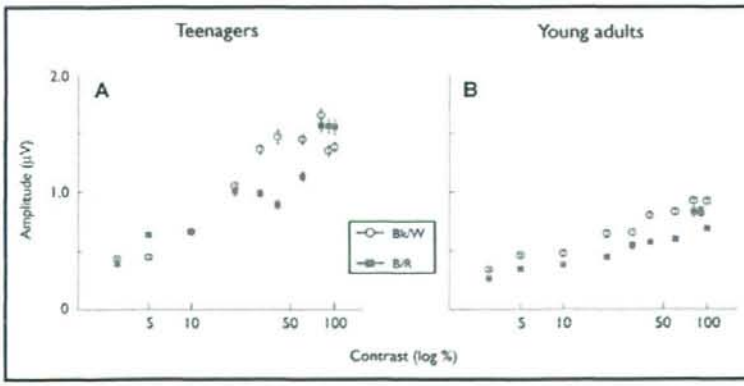

Figure 4.
Contrast modulation functions of VEP amplitudes in response to B/R and Bk/W stimuli at a constant temporal frequency of 12 Hz in teenagers (n = 10) (**A**) and young adults (n = 10) (**B**). Subjects are the same as in Fig. 3. Note that the slopes for the teenagers are much steeper than those for the young adults.
Epilepsia © ILAE

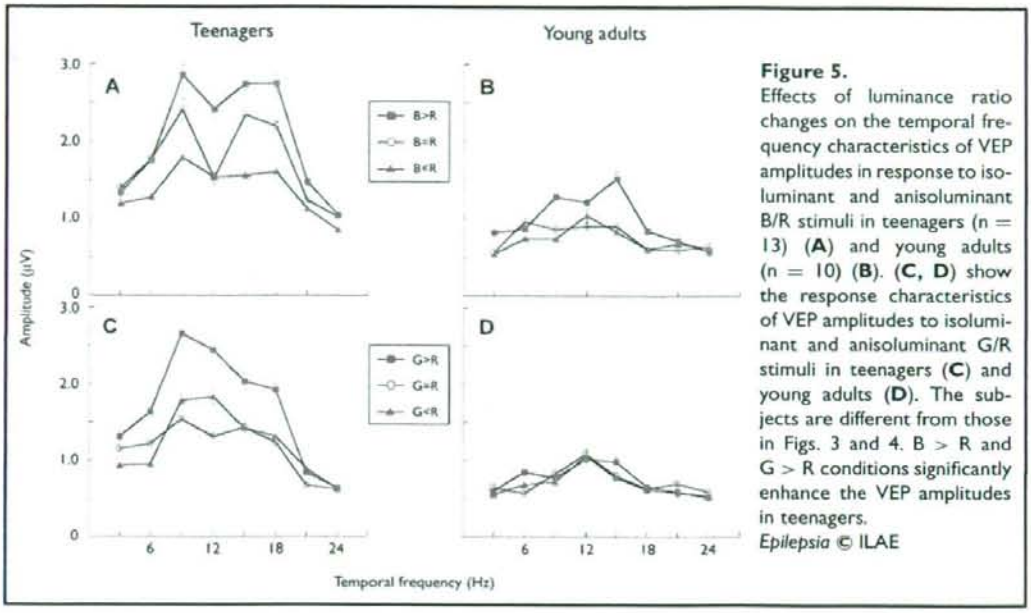

Figure 5.
Effects of luminance ratio changes on the temporal frequency characteristics of VEP amplitudes in response to isoluminant and anisoluminant B/R stimuli in teenagers (n = 13) (**A**) and young adults (n = 10) (**B**). (**C, D**) show the response characteristics of VEP amplitudes to isoluminant and anisoluminant G/R stimuli in teenagers (**C**) and young adults (**D**). The subjects are different from those in Figs. 3 and 4. B > R and G > R conditions significantly enhance the VEP amplitudes in teenagers.
Epilepsia © ILAE

to the activities of the visual cortex but not the retinal cells. Although the lateral geniculate nucleus (LGN) also plays an important role in color processing (Derrington et al., 1984; Horwitz et al., 2005), LGN neurons integrate cone inputs linearly, while the responses of neurons in the visual cortex are nonlinear (Horwitz et al., 2005). Thus, the LGN may not contribute to VEP differences under the isoluminant condition.

Our results raise an important question about the mechanism of the significant changes in photo/chromatic sensitivity around the age of 20 years. There is a significant relationship between the development and aging of the visual cortex and visual function. In the visual cortex, the synaptic density is greatest at 8 months (Regan, 1988), and myelination is complete before 6 years (Benes, 1989; Sowell et al., 2003). Moreover, cell loss is not massive and does not occur rapidly with aging (Spear, 1993; Sowell et al., 2003). Psychophysical and electrophysiological studies also show a gradual decline of visual abilities with aging (Porciatti et al., 1992; Spear, 1993; Fiorentini et al., 1996; Knoblauch et al., 2001; Crognale, 2002). Thus, a drastic change in photo/chromatic sensitivity at around 20 years of age cannot be explained by either continued development or the sudden aging of the visual cortex. On the other hand, lower levels of inhibitory amino acids (GABA, taurine) and higher levels of excitatory amino acids in the cerebrospinal fluid are correlated with increased photosensitivity in photosensitive baboons (Lloyd et al., 1986), and saturation of VEP responses to contrast changes are abolished by local application of bicuculline to the cat visual cortex (Morrone et al., 1987). Considering these results together, we hypothesized that the functional development of inhibitory and excitatory neural networks in the visual cortex may suppress photo/chromatic sensitivity after 20 years of age.

Surprisingly, when the luminance ratio in B/R or G/R stimulation was changed, VEP amplitudes were significantly modulated and the 12-Hz dip became unclear (Fig. 5). These findings suggest that a difference in the luminance of the two colors can influence the activating effect for V1. Color information is perceived by three types of cone in the retina: long (L or red), middle (M or green), and short (S or blue) wavelength-sensitive cones. In monkeys, the color tuning of a population of S cone-driven V1 neurons has been studied (Horwitz et al., 2005). The study suggested the presence of color-luminance interaction in V1; blue (S-cone)-yellow (a combination of L and M cones) color opponent signals are enhanced by a nonopponent signal nonlinearly. Therefore, our finding that VEP amplitudes were modulated by luminance ratio changes may be related to a color-luminance interaction. Moreover, responses to the B/R combination were more enhanced than the G/R combination by luminance contrast in this study. This difference probably results from the absence of an antagonistic effect with B/R but not with G/R stimulation (Livingstone & Hubel, 1984).

VEP amplitudes in both B/R and Bk/W stimuli were significantly increased when contrast was increased. This

result suggests that the responses of the visual cortex to achromatic and chromatic stimuli are modulated by contrast change, and contrast gain control (Spekreijse et al., 1973; Porciatti et al., 2000) is driven in both stimuli. Interestingly, the slopes for teenagers were much steeper than those for the young adults. Thus, achromatic and chromatic contrast sensitivities are higher in teenagers.

Overall, our results suggested latent photo/chromatic sensitivity in adolescence. Is there any link between our findings and PSE? Recent studies (Porciatti et al., 2000; Parra et al., 2003) suggest that there are different mechanisms active in PSE patients compared to healthy subjects, although color sensitivity is an important factor in the generation of PSE (Harding, 1998; Tobimatsu et al., 1999; Parra et al., 2007). Therefore, our results in healthy subjects may not fully explain the neural mechanism of PSE. However, many of those with "Pokemon seizures" had no previous history of epilepsy, and had no recurrence of epileptic seizures in a 5-year follow-up study (Okumura et al., 2004). These facts suggest that the 12-Hz B/R stimulation (luminance ratio; B:R = 4:3) may be a provocative stimulus for the visual cortex to induce seizures in healthy teenagers. This hypersensitivity of the visual cortex to 12-Hz B/R stimulation (luminance ratio; B:R = 4:3) may explain the VEP response characteristics (an unclear 12-Hz dip in the 12 Hz B > R stimulation) in healthy teenagers (Fig. 5).

In conclusion, color-luminance combinations can significantly influence the excitability of the visual cortex. In particular, higher sensitivities to these visual stimuli in teenagers play an important role in photo/chromatic sensitivity in adolescence.

Acknowledgments

This work was supported in part by a grant from the Japan Epilepsy Research Foundation. This study was also supported in part by Grant-in-Aid for the 21st Century COE Program and Grant-in-Aid for Scientists, No. 16390253 and No. 16200005 from the Ministry of Education, Culture, Sports, Science and Technology in Japan.

Conflict of interest: We confirm that we have read the Journal's position on issues involved in ethical publication and affirm that this report is consistent with those guidelines. None of the authors has any conflict of interest to declare.

References

Benes FM. (1989) Myelination of cortical-hippocampal relays during late adolescence. *Schizophr Bull* 15:585–593.

Crognale MA. (2002) Development, maturation, and aging of chromatic visual pathways: VEP results. *J Vis* 2:438–450.

Derrington AM, Krauskopf J, Lennie P. (1984) Chromatic mechanisms in lateral geniculate nucleus of macaque. *J Physiol* 357:241–265.

Fiorentini A, Porciatti V, Morrone MC, Burr DC. (1996) Visual ageing: unspecific decline of the responses to luminance and colour. *Vision Res* 36:3557–3566.

Fisher RS, Harding G, Erba G, Barkley GL, Wilkins A. (2005) Photic- and pattern-induced seizures: a review for the Epilepsy Foundation of America working group. *Epilepsia* 46:1426–1441.

Funatsuka M, Fujita M, Shirakawa S, Oguni H, Osawa M. (2001) Study on photo-pattern sensitivity in patients with electronic screen game-induced seizures (ESGS): effects of spatial resolution, brightness, and pattern movement. *Epilepsia* 42:1185–1197.

Fylan F, Harding GFA. (1997) The effect of television frame rate on EEG abnormalities in photosensitive and pattern-sensitive epilepsy. *Epilepsia* 38:1124–1131.

Harding GFA, Pearce K, Dimitrakoudi M, Jeavons PM. (1975) The effect of coloured intermittent photic stimulation (IPS) on the photoconvulsive response (PCR). *Electroencephalogr Clin Neurophysiol* 39: 428.

Harding GFA, Jeavons PM. (1994) *Photosensitive epilepsy*, new ed. Mac Keith Press, London.

Harding GFA, Jeavons PM, Edson AS. (1994) Video material and epilepsy. *Epilepsia* 35:1208–1216.

Harding GFA. (1998) TV can be bad for your health. *Nat Med* 4:265–267.

Harding GFA, Harding PF. (1999) Televised material and photosensitive epilepsy. *Epilepsia* 40:65–69.

Hayashi T, Ichiyama T, Nishikawa M, Isumi H, Furukawa S. (1998) Pocket Monsters, a popular television cartoon, attacks Japanese children. *Ann Neurol* 44:427–428.

Horwitz GD, Chichilnisky EJ, Albright TD. (2005) Blue-yellow signals are enhanced by spatiotemporal luminance contrast in macaque V1. *J Neurophysiol* 93:2263–2278.

Ishihara S. (1997) *Tests for colour-deficiency*. Kanehara, Tokyo.

Jeavons PM, Harding GFA, Panayiotopoulos CP, Drasdo N. (1972) The effect of geometric patterns combined with intermittent photic stimulation in photosensitive epilepsy. *Electroencephalogr Clin Neurophysiol* 33:221–224.

Kasteleijin-Nolst Trenité DGA. (1998) Reflex seizures induced by intermittent light stimulation. In Zifkin BG, Andermann F, Beaumanoir A, Rowan AJ (Eds) *Reflex epilepsies and reflex seizures: Advance in neurology*. Lippincott-Raven, Philadelphia, pp. 99–121.

Knoblauch K, Vital-Durand F, Barbur JL. (2001) Variation of chromatic sensitivity across the life span. *Vision Res* 41:23–36.

Livingstone MS, Hubel DH. (1984) Anatomy and physiology of a color system in the primate visual cortex. *J Neurosci* 4:309–356.

Lloyd KG, Scatton B, Voltz C, Bryere P, Valin A, Naquet R. (1986) Cerebrospinal fluid amino acid and monoamine metabolite levels of Papio papio: correlation with photosensitivity. *Brain Res* 363:390–394.

Marmor MF, Holder GE, Seeliger MW, Yamamoto S. (2004) Standard for clinical electroretinography (2004 update). *Doc Ophthalmol* 108:107–114.

Morrone MC, Burr DC, Speed HD. (1987) Cross-orientation inhibition in cat is GABA mediated. *Exp Brain Res* 67:635–644.

Okumura A, Watanabe K, Ishikawa T. (2004) Five years after the "Pocket Monster" seizures. *N Engl J Med* 351:403–404.

Panayiotopoulos CP, Jeavons PM, Harding GFA. (1972) Occipital spikes and their relation to visual evoked responses in epilepsy, with particular reference to photosensitive epilepsy. *Electroencephalogr Clin Neurophysiol* 32:179–190.

Parra J, Kalitzin SN, Iriarte J, Blanes W, Velis DN, Lopes da Silva FH. (2003) Gamma-band phase clustering and photosensitivity: is there an underlying mechanism common to photosensitive epilepsy and visual perception? *Brain* 126:1164–1172.

Parra J, Kalitzin SN, Stroink H, Dekker E, de Wit C, Lopes da Silva FH. (2005) Removal of epileptogenic sequences from video material: the role of color. *Neurology* 64:787–791.

Parra J, Lopes da Silva FH, Stroink H, Kalitzin S. (2007) Is colour modulation an independent factor in human visual photosensitivity? *Brain* 130:1679–1689.

Porciatti V, Burr DC, Morrone MC, Fiorentini A. (1992) The effects of ageing on the pattern electroretinogram and visual evoked potential in humans. *Vision Res* 32:1199–1209.

Porciatti V, Bonanni P, Fiorentini A, Guerrini R. (2000) Lack of cortical contrast gain control in human photosensitive epilepsy. *Nat Neurosci* 3:259–263.

Regan D. (1988) *Human brain electrophysiology. Evoked potentials and evoked magnetic fields in science and medicine*. Elsevier, New York.

Sowell ER, Peterson BS, Thompson PM, Welcome SE, Henkenius AL, Toga AW. (2003) Mapping cortical change across the human life span. *Nat Neurosci* 6:309–315.

Spear PD. (1993) Neural bases of visual deficits during aging. *Vision Res* 33:2589–2609.

Spekreijse H, Van der Twell LH, Zuidema T. (1973) Contrast evoked responses in man. *Vision Res* 13:1577–1601.

Takahashi T. (2002) *Photosensitive epilepsy*. Igaku-Shoin, Tokyo.

Tobimatsu S, Zhang YM, Tomoda Y, Mitsudome A, Kato M. (1999) Chromatic sensitive epilepsy: a variant of photosensitive epilepsy. *Ann Neurol* 45:790–793.

Wilkins AJ, Darby CE, Binnie CD, Stefansson SB, Jeavons PM, Harding GFA. (1979) Television epilepsy-the role of pattern. *Electroencephalogr Clin Neurophysiol* 47:163–171.

ELSEVIER

Clinical Neurophysiology 119 (2008) 1803–1811

www.elsevier.com/locate/clinph

Electrophysiological evidence for sequential discrimination of positive and negative facial expressions

T. Nakashima[a,f,*], Y. Goto[a,d], T. Abe[b], K. Kaneko[c], T. Saito[a], A. Makinouchi[e], S. Tobimatsu[a]

[a] *Department of Clinical Neurophysiology, Neurological Institute, Faculty of Medicine, Graduate School of Medical Sciences, Kyushu University, 3-1-1 Maidashi, Fukuoka 812-8582, Japan*

[b] *Graduate School of Systems Life Sciences, Kyushu University, Fukuoka, Japan*

[c] *Department of Intelligent Systems, Graduate School of Information Science and Electrical Engineering, Kyushu University, Fukuoka, Japan*

[d] *Department of Occupational Therapy, Faculty of Rehabilitation, International University of Health and Welfare, Okawa, Japan*

[e] *Department of Information and Network Engineering, Kurume Institute of Technology, Kurume, Japan*

[f] *Japan Society for the Promotion of Science (JSPS), Tokyo, Japan*

Accepted 17 April 2008
Available online 5 June 2008

Abstract

Objective: To elucidate the differences in temporal processing between positive and negative facial expressions by using event-related potentials (ERPs) with spatially filtered images.

Methods: Based on the traits of parallel visual pathways, four types of facial expression images (happiness, fear, anger and neutral) with low, high and broadband spatial frequencies (LSF, HSF and BSF, respectively) were carefully created with the consideration of luminance, contrast and emotional intensity. These images were pseudo-randomly presented to 13 healthy subjects to record ERPs. Twenty recording electrodes were placed over the scalp according to the International 10–20 system. For emotion-relevant late negative components with latencies of 190–390 ms, the amplitude differences among the four facial expressions were analyzed for sequential 20-ms time windows by ANOVA.

Results: There were significant amplitude differences between positive and negative LSF facial expressions in the early time windows of 270–310 ms at the occipitotemporal region. Subsequently, the amplitudes among negative HSF facial expressions differed significantly in the later time windows of 330–390 ms.

Conclusions: Discrimination between positive and negative facial expressions precedes discrimination among different negative expressions in a sequential manner based on parallel visual channels.

Significance: ERPs with spatially filtered images have provided the first evidence for sequential discrimination of positive and negative facial expressions.

© 2008 International Federation of Clinical Neurophysiology. Published by Elsevier Ireland Ltd. All rights reserved.

Keywords: Event-related potentials; Positive and negative facial expressions; Parallel visual channels; High and low spatial frequencies

1. Introduction

Facial expression recognition is one of the most important skills in social communications. In everyday life, we can readily identify individuals, as well as the age and gender of faces, without difficulty. Humans are even able to guess someone's emotions from their facial expressions at a particular moment. However, patients with autism spectrum disorders and schizophrenia often show behavioral patterns that differ from the usual patterns for these cognitive activities, and thus have a disadvantage in daily social communications (Elger and Campbell, 2001). Therefore, elucidating the brain mechanisms involved in facial expression recognition may lead to the development of therapeutic interventions.

* Corresponding author. Address: Department of Clinical Neurophysiology, Neurological Institute, Faculty of Medicine, Graduate School of Medical Sciences, Kyushu University, 3-1-1, Maidashi, Fukuoka 812-8582, Japan. Tel.: +81 92 642 5543; fax: +81 92 642 5545.
E-mail address: taisuke@med.kyushu-u.ac.jp (T. Nakashima).

1388-2457/$34.00 © 2008 International Federation of Clinical Neurophysiology. Published by Elsevier Ireland Ltd. All rights reserved.
doi:10.1016/j.clinph.2008.04.014

A number of studies have indicated that the amygdala is engaged in processing facial expressions, especially fearful expressions (Morris et al., 1998; Adolphs, 2002; Posamentier and Abdi, 2003). Several ERP studies have reported that the late components (180–750 ms) are related to facial expression processing (Streit et al., 2000; Sato et al., 2001; Krolak-Salmon et al., 2001; Eimer and Holmes, 2002; Balconi and Pozzoli, 2003; Schupp et al., 2004; Ashley et al., 2004). However, the scalp distributions and peak latencies of these slow late components are inconsistent among the studies. Moreover, direct functional correlations between late ERP components and the amygdala can be difficult to estimate. Therefore, the neural basis for the spatiotemporal characteristics of the late ERP components for discriminating various facial expressions has not yet been clarified.

A recent functional MRI study (Vuilleumier et al., 2003) revealed that low spatial frequency (LSF) images of a fearful expression activated the amygdala to a much greater extent than unfiltered images (broadband spatial frequency, BSF). In contrast, high spatial frequency (HSF) images of a neutral face mainly activated the fusiform gyrus compared with LSF faces. These observations are supported in part by the physiological traits of two parallel visual pathways. Specifically, the magnocellular (M) stream mainly analyzes coarse (or LSF) information and sends rapid visual signals to the amygdala via the tecto-pulvinar pathway (Schiller et al., 1979; Liddell et al., 2005), while slower visual signals with fine spatial (or HSF) information are chiefly projected to ventral cortical areas such as the fusiform gyrus via the parvocellular (P) stream (Livingstone and Hubel, 1988; Tobimatsu and Celesia, 2006). Since the study by Vuilleumier et al. (2003), several investigators have recorded ERPs to determine the effects of SF on face or facial expression perception by measuring the early P1 and face-sensitive N170 (Goffaux et al., 2003; Pourtois et al., 2005; Holmes et al., 2005; Halit et al., 2006). It has been suggested that LSF information plays an important role in the recognition of faces or facial expressions (especially fearful faces) in the early P1 and N170 (Goffaux et al., 2003; Pourtois et al., 2005; Halit et al., 2006). However, the importance of HSF information for M170, a counterpart of N170, was reported in a magnetoencephalographic study (Hsiao et al., 2005). It is also noteworthy that N170 was not affected by SF information (Holmes et al., 2005). To date, no reports have demonstrated how the late components behave differently and process HSF and LSF information of facial expressions.

The discrepant results for the P1 and N170 components among previous ERP studies may arise from methodological differences and/or differences between the SF cut-off values used to create the filtered faces. Briefly, the subjects' task-relevant attention to faces can be a critical factor that affects the ERP components, especially the late components (Krolak-Salmon et al., 2001). Nevertheless, face-relevant attentive tasks, such as the gender decision task and face categorization task, have often been employed (Goffaux et al., 2003; Pourtois et al., 2005; Halit et al., 2006). The definitions of LSF and HSF are quite different among previous studies, ranging from <5 to 8 cycles/face for LSF and >15 to 32 cycles/face for HSF (Goffaux et al., 2003; Pourtois et al., 2005; Holmes et al., 2005; Hsiao et al., 2005; Halit et al., 2006). These cut-off values did not take into account whether the subjects could precisely recognize the facial effects for each facial expression. In addition, the physical characteristics of the filtered photographs, such as luminance and contrast, were not strictly controlled.

On the other hand, psychological developmental studies have revealed that infants prefer looking at happy faces compared with angry or neutral faces (LaBarbera et al., 1976) and vice versa (Nelson and Dolgin, 1985). In addition, infants can distinguish happy faces from fearful faces (Nelson et al., 1979). These findings suggest that recognition of happiness and fear is essential for our early life. Infants have low vision compared with adults and rely more heavily on LSF information. Furthermore, the judgment speeds for happiness are faster than those for negative facial expressions in adults (Kirouac and Dore, 1983). Therefore, we hypothesized that discrimination between positive and negative expressions first occurs in the late components, even in healthy adults, via LSF information. Subsequently, more detailed analyses among other expressions occur via HSF information.

To test this hypothesis, we recorded ERPs to positive and negative expressions (anger, fear, happiness and neutral) using BSF, LSF and HSF facial expressions created by image engineering. Prior to the ERP study, we determined the psychophysical thresholds (cut-off values for SF) of facial expression recognition to equalize the subjective intensity for each expression (Fig. 1). Thus, our filtered face stimuli were uniquely created with consideration of the luminance contrast of the faces and facial expressions, and the physical factors and facial expression intensities were equated. We also employed a simple passive viewing task with a target stimulus (shoes) to maintain the subjects' vigilance and attentional direction away from the facial expressions. Using such a careful approach, we predicted that the late components would show characteristic changes in the amplitudes or latencies of the late components (e.g., an amplitude increase and a latency decrease) for each filtered positive and negative facial expression, and that such alterations would provide new insights into the neural mechanisms of social cognition in humans.

2. Methods

2.1. Subjects

The study participants were 13 healthy undergraduate students with normal or corrected to normal vision (6 females and 7 males; age range, 21–25 years; mean age, 22.4 years) who were naive to our experimental stimuli. They did not have any history of neurological or psychiatric disorders. The subjects were paid for their participation and signed informed consent after the nature of the exper-

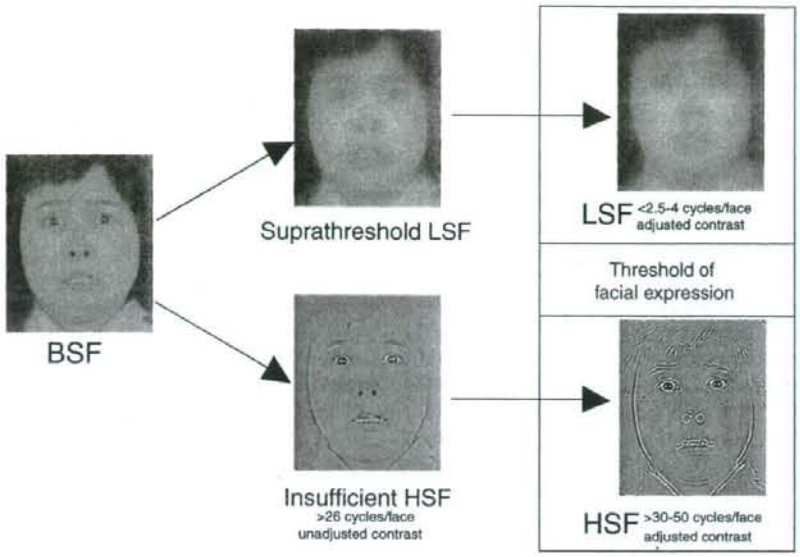

Fig. 1. Representative examples of the fearful stimuli used in the present study. BSF is an original non-filtered image (left), which contains broad spatial frequency components. LSF and HSF faces are filtered by fast Fourier transformation. The middle column shows inadequate stimuli. Insufficient HSF is caused by using a lower cut-off point and not adjusting the contrast, such that the HSF component of the image is not fully enhanced. Suprathreshold LSF is too easy to recognize and similar to the BSF condition, such that the effects of LSF on the ERPs are not disclosed by these stimuli. Therefore, these stimuli are not suitable for our ERP experiments. The right column shows our preferred stimuli. The threshold for recognizing facial expressions was measured by psychophysical experiments in advance, and the contrast of the images was adequately normalized. The LSF face consists of information with low spatial frequencies (<2.5–4 cycles/face width) and preserves the holistic facial image. The HSF face extracts information with high spatial frequencies (>30–50 cycles/face width) and emphasizes the detailed features of the facial components.

iments had been fully explained. The local Ethics Committee of Kyushu University approved the study.

2.2. Original stimuli

The original stimuli were 256-level grayscale photographs of emotional (angry, fearful and happy) and neutral faces taken from Japanese and Caucasian Facial Expressions of Emotion (JACFEE) and Neutral Faces (JACNeuF), respectively (Matsumoto and Ekman, 1988). Although JACFEE and JACNeuF consisted of four Japanese photos for each expression, we only used two photographs for each facial expression (1 male and 1 female) because the other photographs were not appropriately evaluated as portraying the intended emotion by our subjects in preliminary experiments.

To control the subjects' attention and vigilance, a target stimulus (shoes) was taken from our own 256-level grayscale photographs.

2.3. Manipulation of stimuli

LSF and HSF stimuli for faces and houses were created by image engineering techniques with two-dimensional fast Fourier transformation (one-order Gaussian window method for LSF; 35-order Hamming window method for HSF) using our own program written in C language and MATLAB ver. 7 (The MathWorks Inc.). The BSF stimuli were original photographs and left unfiltered. The mean cut-off frequencies (<2.5–4.0 cycles/face for LSF; >30.0–50.0 cycles/face for HSF) were determined by measuring the psychophysical thresholds for recognition of facial expressions using 30 other recruited subjects (10 females and 20 males; age range, 20–34 years; mean age, 25.7 years; unpublished data) prior to the ERP recordings (Table 1). We did not allow these subjects to participate in the ERP experiments because they were habituated by the repeated exposures of the filtered facial expressions and a repetition effect of upright faces on the brain activity at ~250 ms has been reported (Schweinberger et al., 2007).

In this experiment, we presented 20 levels of filtered photographs in descending series (LSF: from 1.0 to 17.0 cycles/face width; HSF: from 6.0 to 126.0 cycles/face width) and asked the subjects to choose the appropriate emotion from six basic emotions. The recognition thresholds for each category were determined as the first images when the subjects consecutively responded with successful answers. In general, none of the subjects recognized differences in the SF among the facial expressions despite the difference in threshold frequency for each facial expression condition. Although the cut-off values showed slight variability among the different facial expressions, they were approximately the same as those in a previous study using spatially filtered images (Vuilleumier et al., 2003). The images of all the faces were trimmed

Table 1
Mean (±SEM) recognition thresholds for each expression stimuli (cycles/face width) ($n = 30$)

SF	Gender	Anger	Fear	Happiness	Neutral
LSF	Male	3.8 ± 1.0	4.9 ± 1.7	2.4 ± 0.2	5.0 ± 0.9
	Female	4.4 ± 1.8	3.7 ± 0.7	2.5 ± 0.3	5.3 ± 1.0
HSF	Male	38.4 ± 4.6	30.8 ± 2.5	50.0 ± 3.7	38.4 ± 3.2
	Female	32.8 ± 3.7	36.9 ± 4.7	50.8 ± 4.1	41.2 ± 3.1

into rectangles in accordance with the face width, and adjusted to 512 × 614 pixels. If the contrast of HSF images was not adjusted, these images became relatively low-contrast stimuli because the original power of the HSF information of the natural images was low (Fig. 1, lower middle) and the evoked responses would therefore be reduced. Our HSF stimuli were strictly adjusted to ensure that the LSF and HSF images had the same extents of contrast (Fig. 1, right column). We also used high-order filtering (35 orders) to enhance the HSF information and exclude the LSF information more clearly. In other words, the high-order window method helped us to extract the HSF components more strictly. The mean luminance and contrast were controlled by normalizing the mean and standard deviation (SD) of the gray values of all the stimuli using our own program written in C language (mean luminance, 48 cd/m^2; mean gray value ±SD, 128 ± 40). Representative examples of the stimuli (fearful expression) are shown in Fig. 1. Moreover, images of gray value 128 (1024 × 768) were added to all the stimuli as a background. Representative examples of the other facial expressions under each SF condition are shown in Fig. 2.

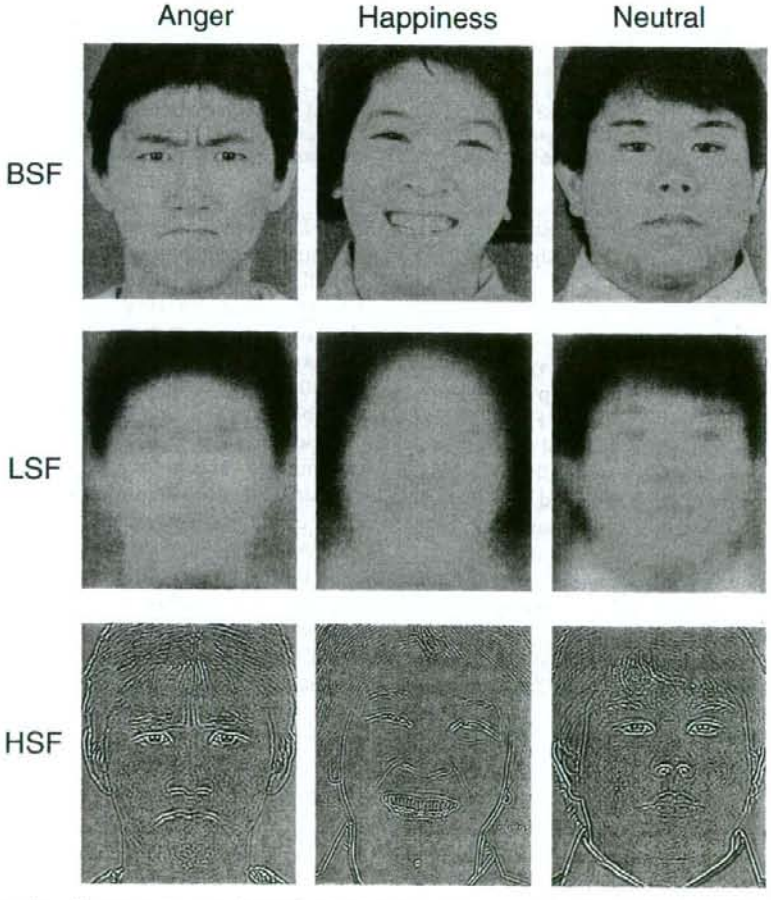

Fig. 2. Representative examples of the angry, happy and neutral stimuli used in the present study. The details for the BSF, LSF and HSF images are described in the legend to Fig. 1.

2.4. Task

The subjects viewed all the stimuli presented on a 17-in. computer screen (Sony Trinitron GT200; refresh rate, 100 Hz; 1024 × 768 pixels) in a dark room. Each facial emotion, except for the target stimulus (shoes), was presented pseudo-randomly under each SF condition for 300 ms with an inter-stimulus interval (ISI) of 700 ms on the computer screen at a viewing distance of 114 cm (visual angle, 8.3 × 10.0 degrees) under the control of VSG 2/5 (Cambridge Research System Co.). The subjects were instructed to fixate on a point in the center of the screen and push a button when a target stimulus (shoes, 10% probability) appeared but ignore other stimuli. The target stimulus was used for controlling the attention and maintaining the vigilance of the subjects. The visual stimuli were replaced by the background image (1024 × 768 pixels) of gray value 128 during the ISI. The reaction time (RT) and accuracy for the target stimulus were also measured while recording the ERPs.

2.5. ERP recording

Silver–silver chloride electrodes were applied to 20 scalp sites on the basis of the International 10–20 system (Fp1, Fp2, Fz, F3, F4, F7, F8, Cz, C3, C4, T3, T4, Pz, P3, P4, T5, T6, Oz, O1 and O2) with collodion. All the recording electrodes were referred to an electrode at the nose-tip, and the impedance was kept below 5 kΩ. Vertical and horizontal electrooculograms (V-EOG and H-EOG, respectively) were also recorded in order to reject artifacts caused by blinking and eye movements. A trigger pulse was generated at the onset of each stimulus. A total of 220 responses were averaged for each stimulus with a band-pass filter between 0.05 and 200 Hz. For visualization of the late components, a 70-Hz high-cut filter was applied. The sampling rate was 1333 Hz, and the recording time for each stimulus was 768 ms. A baseline was set from −72 ms to the onset of the stimuli (0 ms). Artifact rejections were conducted manually on the basis of deflections above 30 μV from the baseline. As a result, the mean rejection rate was 30.8%.

After the ERP recordings, the subjects participated in an unstructured interview with one of the authors (TN) and were asked to state as many as possible of the kinds of facial images they recognized. However, we did not measure the psychophysical thresholds for the recognition of each facial stimulus or the difference in valence between positive and negative expressions before the experiment in order to avoid the repetition effect of upright faces on the brain activity at ~250 ms (Schweinberger et al., 2007) and the task-relevant attention to faces (Krolak-Salmon et al., 2001).

2.6. Data analysis and statistics

The amplitudes of the late components were calculated by averaging the values of 20-ms time windows from 190 to 390 ms at the occipitotemporal regions (T5, T6), since previous studies detected different ERP activation patterns between facial identification and facial expression recognition tasks with unfiltered photographs at these electrodes (Bentin et al., 1996; Sato et al., 2001; Krolak-Salmon et al., 2001).

Statistical analysis was conducted by four-way repeated-measures analysis of variance (ANOVA) (spatial frequency (BSF, LSF or HSF) × 20-ms time windows (190–210, 210–230, 230–250, 250–270, 270–290, 290–310, 310–330, 330–350, 350–370 or 370–390 ms) × laterality (T5 or T6) × facial expression (anger, fear, happiness or neutral)) with the Huynh–Feldt correction for degrees of freedom. As a post hoc analysis, multiple paired comparisons (Bonferroni) were conducted for each time window under each SF condition to focus on the effects of SF on facial expressions in the late components in each time window. All statistical analyses were performed using SPSS 11.01 (SPSS Inc.).

3. Results

3.1. Preliminary psychological experiment

The mean (±SEM) SF thresholds for recognition of facial expressions are shown in Table 1. The mean cut-off frequency for each filtered facial expression was used as the visual stimulus for the ERP recordings in the separate group.

3.2. Psychological evaluation after ERP recordings

All the subjects reported that they perceived at least two kinds of negative expressions (i.e., anger and fear), a positive expression (happy) and neutral faces for all of the filtered conditions.

3.3. Performance of target detection during ERP recordings

The mean (±SD) reaction time for the target stimulus (shoes) was 386.8 ± 31.5 ms, and the correct detection rate (±SD) was 99.9 ± 0.1%. The P300 ERP component was recorded in all subjects with this high performance. N170, a hallmark of face identification, was predominantly recorded over the occipitotemporal sites (T5 and T6) (Fig. 3). However, we did not find any significant effects of SF on this component. The high detection rate indicates that the subjects were alert and that their attention was well controlled during the ERP recordings.

3.4. Late components differentiate positive–negative and negative–negative expressions

Late components were found at the T5 and T6 electrodes. Fig. 4 shows enlarged waveforms of the late components for LSF, BSF and HSF faces at T5 and T6 for the time window of 200–450 ms. Significant main effects of SF, time window and laterality were observed

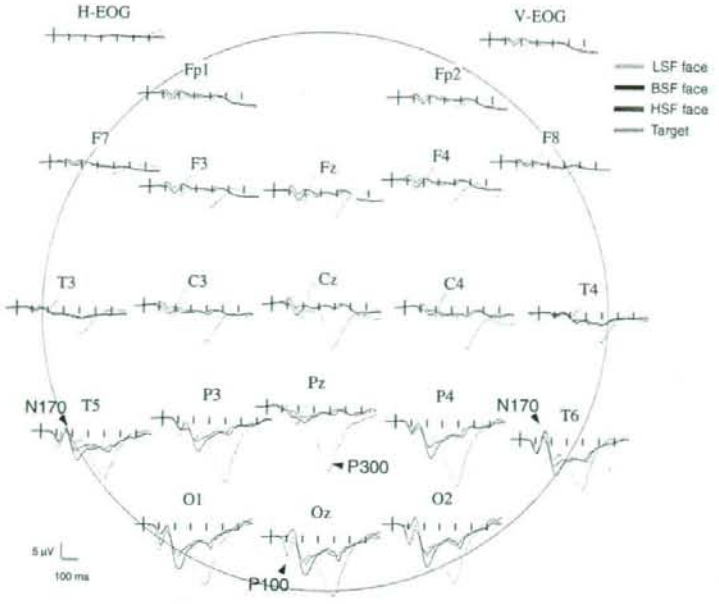

Fig. 3. Topographical mapping of grand-averaged ERPs to the face and target stimuli. Note that P300 is only clearly recorded for the target stimulus.

($F(1.615, 19.375) = 4.501$, $p < 0.05$, $F(2.500, 30.004) = 7.253$, $p < 0.005$ and $F(1,12) = 8.513$, $p < 0.05$, respectively). A significant three-way interaction of SF × time window × facial expression was also found ($F(15.401, 184.812) = 5.121$, $p < 0.001$). The colored boxes in Fig. 3 illustrate significant amplitude differences among facial expressions following the post hoc test of the three-way interaction. The LSF happy faces induced significant negative shifts of the potential compared to negative expressions (anger, fear) in the early time windows (270–290 and 290–310 ms) ($p < 0.05$). In contrast, the HSF fearful faces elicited significant negative shifts of the potential compared to angry faces in the later time windows (330–350, 350–370 and 370–390 ms) ($p < 0.05$). No significant amplitude differences were observed for neutral faces (Fig. 4). It is important to note that we did not find any significant effects for facial expressions under the BSF condition.

In summary, LSF images induced different responses between positive and negative expressions (anger/fear vs. happiness) in the relatively early phase of the late components, while HSF images elicited significant differences in the amplitudes among different negative expressions (anger vs. fear) in the late phase of the late components.

4. Discussion

4.1. Importance of SF for discrimination between positive and negative expressions

The present study examined the influence of SF filtering on brain processing of affective facial photographs. To manipulate the SF characteristics of the stimuli, the photographs were presented without filtering (BSF), after low-pass filtering to retain only LSF components (<2.5–4.0 cycles/face width) or after high-pass filtering to retain only HSF components (>30.0–50.0 cycles/face width). As a result, different effects of LSF and HSF information on the late components were clearly demonstrated, while BSF had no significant effects on the late components. These results suggest that modulation of the SF information is a critical factor that influences the behaviors of the late components.

The amplitudes within 270–310 ms (N270–310) differed significantly among happiness and fear/anger in the LSF condition, while the amplitudes within 330–390 ms (N330–390) differed significantly between anger and fear in the HSF condition. These findings suggest that discrimination of a positive expression from a negative expression occurs in the early phase of the late components, while discrimination among negative expressions is achieved in a much later phase of the late components. These interpretations are supported by a behavioral study in which the latency of judgment of a happy expression was earliest, while those of angry and fearful expressions were last (Kirouac and Dore, 1983). The early components (from P1 to 150 ms) were significantly modulated by LSF fearful faces (Pourtois et al., 2005), which may be related to early detection of a threat. However, we did not find any effects of SF on facial expressions in these time windows. Therefore, our late components may not reflect the first detection of emotional content but rather the processing of detailed emotional contents.

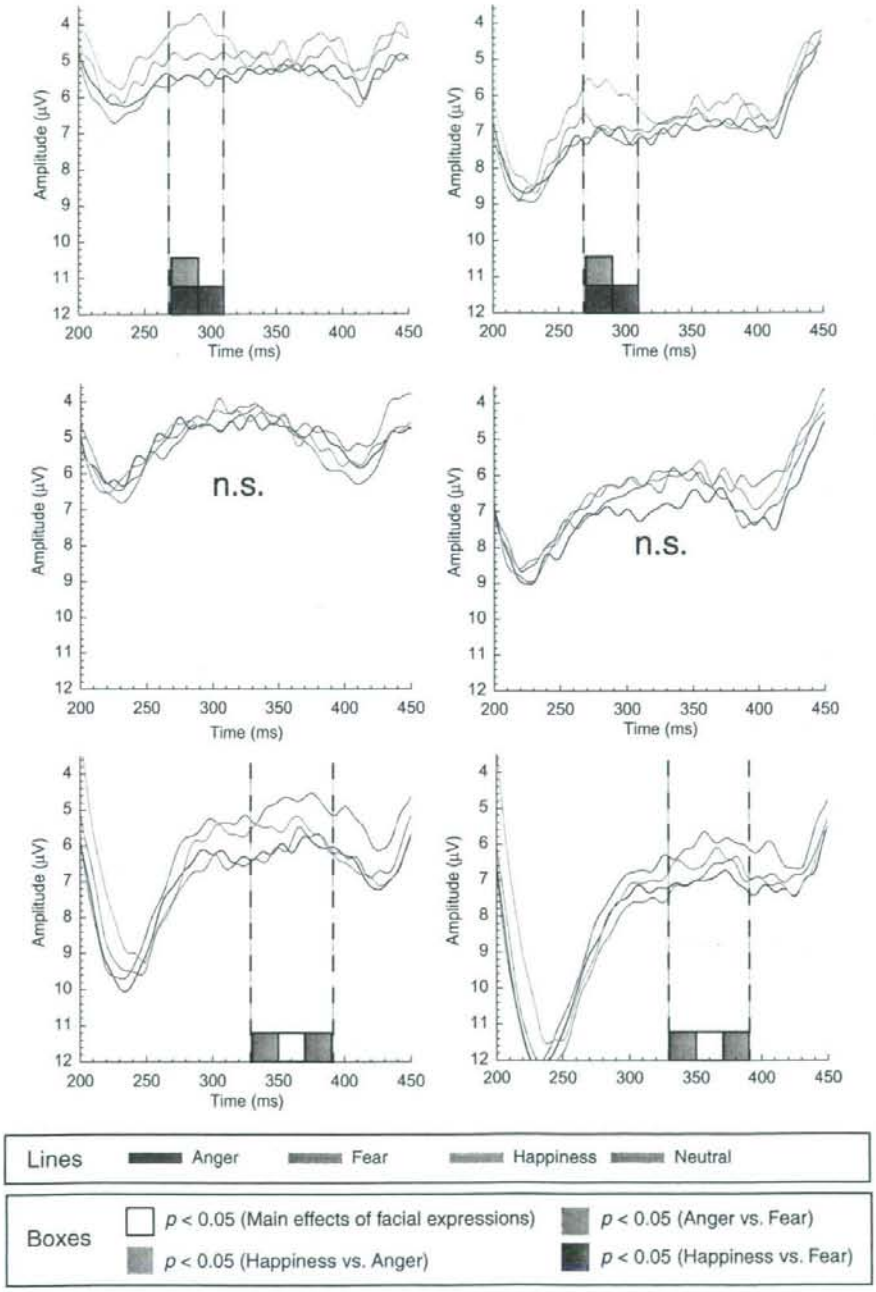

Fig. 4. Waveforms of the late components for the facial expressions of each stimulus. The preceding N170 is omitted while the time window of 200–450 ms is enlarged for comparison. The white square boxes on the abscissa indicate main effects of facial expressions, while the colored boxes show statistically significant differences revealed by paired comparisons (Bonferroni correction). Under the LSF condition, there are significant differences in the amplitudes between positive (happiness) and negative (anger or fear) expressions during the time window of 270–310 ms, regardless of the hemisphere. In contrast, a significant difference is found among negative expressions (anger vs. fear) during the time window of 330–390 ms under the HSF condition.

4.2. Insignificant contribution of unfiltered images to the late components

Although naturalistic (BSF) images of faces provide both LSF and HSF information simultaneously, there were no significant differences in the late components among the facial expressions under the BSF condition. In the present study, the attention of the subjects was directed toward the target stimulus (shoes), and the influence of attention to the facial ERPs was therefore relatively small compared with direct attention tasks to facial stimuli. Krolak-Salmon et al. (2001) reported that there were no significant differences in the amplitudes among facial expressions when the subjects did not pay direct attention to the facial expressions themselves. Similarly, Vuilleumier et al. (2003) did not find any significant effects for BSF stimuli in a gender identity task using functional MRI. In addition, we determined the psychophysical thresholds (cut-off values for SF) of facial expression recognition in a separate group of subjects to equalize the subjective intensity for each facial expression, since the psychophysical threshold of mosaic faces was found to have a significant effect on face recognition in our previous study (Goto et al., 2005). Overall, the expression intensity of our stimuli and attention had no significant influences on the late components under the BSF condition. Therefore, only the SF information is an important factor that affected the late components.

4.3. Neural basis for sequential processing of facial expressions

Our results provide evidence that processing of facial expressions is enhanced by SF modulation and processed sequentially over time by using LSF and HSF information in conjunction. We hypothesize that enhancing either the LSF or HSF components of faces can alert the M and P pathways contingently, which in turn facilitate information processing in the human brain to discriminate among facial expressions. Indeed, brain structures sensitive to emotionally relevant information such as the amygdala, superior colliculus and pulvinar, part of a phylogenetically old route specialized for rapid processing of fear-related stimuli, appear to be preferentially activated by LSF information, but not HSF information, via the fast M pathway (Vuilleumier et al., 2003; Winston et al., 2003; Liddell et al., 2005; Eimer and Holmes, 2007). In contrast, the slow P pathway, which is more responsive to HSF stimuli, provides input to the ventral visual cortex such as the fusiform gyrus, but not to subcortical areas, and is crucial for detailed processing of the shape of the visual object (Livingstone and Hubel, 1988; Tobimatsu and Celesia, 2006). Therefore, it is plausible that the N270–310 component uses LSF information via the M pathway and rapidly segregates positive and negative expressions. Subsequently, the N330–390 component utilizes HSF information via the P pathway and differentiates among negative expressions in more detail. Interestingly, Goren and Wilson (2006) recently demonstrated that recognition of happiness was robust even if happy faces were presented in the peripheral vision. Since the M pathway handles information processing from the peripheral visual field, their finding is consistent with our result that the behavior of the N270–310 component under the LSF condition reflects a discriminative stage between positive and negative expressions.

To date, the neural generators of the late components have remained controversial. Although it is possible that many cortical structures contribute to the late components observed in our study, especially for happy expressions, previous reports had suggested that the visual cortices are activated by the distant influence of the amygdala when subjects recognize facial expressions (Morris et al., 1998; Vuilleumier et al., 2004). In addition, Amaral et al. (2003) proved the existence of direct connections from the amygdala to the visual cortices. Therefore, it is possible that the positive shifts in the early late components for LSF fearful faces compared to LSF happy faces may result from a re-entrance projection from the amygdala or various other cortico-subcortical regions related to emotional processing (Sato et al., 2001).

4.4. Methodological considerations

Care was taken to create the spatially filtered images in this study. However, because we did not measure the psychophysical data for each stimulus before the ERP experiment, which subjects actually recognized the facial valence (negative, positive) on a single trial basis might be debatable. We sought to avoid the repetition effects of facial expressions on ERPs (Schweinberger et al., 2007); however, such effects can arise while measuring ERPs. Future research needs to include concurrent measures of psychophysical data and ERP recordings in the same subjects. This should provide additional information on SF/valence interaction effects in the late components.

5. Conclusions

We have found for the first time that positive and negative facial expressions are processed sequentially over time based on the traits of parallel visual pathways. Specifically, the early late component within 270–310 ms reflects the discrimination between positive and negative expressions depending on LSF information, while the subsequent late component within 330–390 ms reflects the discrimination among different negative expressions based on HSF information.

Acknowledgements

We thank Professor G.G. Celesia (Department of Neurology, Loyola University Medical Center, Maywood, IL) for his critical comments regarding this manuscript. We thank Professor H. Sakamoto (Department of Visual Com-